RNAAS RESEARCH NOTES OF THE AAS

Examining the Rotation of the Planet-hosting M Dwarf GJ 3942

To cite this article: Andrew Fonseca and Sarah Dodson-Robinson 2024 *Res. Notes AAS* **8** 291

Draft version November 22, 2024
Typeset using LaTeX default style in AASTeX631

Examining the rotation of the planet-hosting M dwarf GJ 3942

Andrew Fonseca[1] and Sarah Dodson-Robinson[1]

[1] *University of Delaware*
Newark, DE 19716, USA

ABSTRACT

Based on radial velocities, EXORAP photometry, and activity indicators, the HADES team reported a 16.3-day rotation period for the M dwarf GJ 3942. However, an estimate of the magnitude-squared coherence between the HADES RV and Hα time series has significant peaks at frequencies 1/16 day^{-1} and 1/32 day^{-1}. We turn to TESS photometry to test the hypothesis that the true rotation period is 32 days with 16-day harmonic. Although the average TESS periodogram has peaks at harmonics of 1/16 day^{-1}, the harmonic sequence is not fully resolved according to the Rayleigh criterion. The TESS observations suggest a 1/16 day^{-1} rotation frequency and a 1/32 day^{-1} subharmonic, though resolution makes the TESS rotation detection ambiguous.

Keywords: Stellar Rotation (1629) — Stellar activity (1580) — Radial Velocity (1332) — Period search (1955) — Lomb-Scargle periodogram (1959) — Time Series Analysis (1916)

1. INTRODUCTION

GJ 3942, an M0.5V star (Lépine et al. 2013) at a distance of 16.9 pc (Gaia Collaboration 2020), is a HArps-n red Dwarf Exoplanet Survey (HADES) target with 145 high-resolution spectra obtained over 1203 nights. In addition to planet GJ 3942 b, Perger et al. (2017a) also found 16.3-day periodicity in the RV, S-index, Hα, and EXOplanetary systems Robotic APT2 Photometry time series that they attributed to star rotation. We investigated the rotation signal using published HADES data and TESS photometry.

2. MAGNITUDE-SQUARED COHERENCE BETWEEN RV AND ACTIVITY INDICATORS

Oscillations that jointly manifest in RVs and activity indicators are caused by stellar activity, not by planets. We detect such oscillations by estimating magnitude-squared coherence $\hat{C}^2_{xy}(f)$, which is a frequency-dependent correlation coefficient between activity-indicator time series x_t and RV time series y_t:

$$\hat{C}^2_{xy}(f) = \frac{\sum_{k=0}^{K-1} |\hat{S}^{(k)}_{xy}(f)|^2}{\left(\sum_{k=0}^{K-1} \hat{S}^{(k)}_{xx}(f)\right)\left(\sum_{k=0}^{K-1} \hat{S}^{(k)}_{yy}(f)\right)}. \quad (1)$$

In Equation (1), f is frequency, x_t and y_t are broken into K segments, $\hat{S}^{(k)}_{xx}(f)$ and $\hat{S}^{(k)}_{yy}(f)$ are estimated power spectra of x_t and y_t from segment k, and $\hat{S}^{(k)}_{xy}(f)$ is the estimated cross-spectrum of x_t and y_t from segment k (e.g. Percival & Walden 2020). A statistically significant peak in $\hat{C}^2_{xy}(f)$ suggests that stellar activity generates the RV oscillation at frequency f (Dodson-Robinson et al. 2022).

Figure 1 (top left) shows $z(f)$, a Fisher (1929) transformation of $\hat{C}^2_{xy}(f)$ computed with x_t = Hα index (Gomes da Silva et al. 2011), y_t = RV from the TERRA pipeline (Anglada-Escudé & Butler 2012), and each time series broken into two overlapping segments (Welch 1967) and tapered with four-term Blackman-Harris windows (Harris 1978). Shared oscillations nearly reach the 0.1% false alarm level at $f = 1/16$ day^{-1}, the rotation signal reported by Perger et al. (2017a), and $f = 1/32$ day^{-1}. The $f = 1/32$ day^{-1} signal also appears in an RV power spectrum estimate.

afonse@udel.edu, sdr@udel.edu

Star rotation often produces periodogram peaks at harmonic frequencies in addition to the fundamental (e.g. Boisse et al. 2011; Ramiaramanantsoa et al. 2018). We turn to TESS photometry to investigate whether GJ 3942 might have a true rotation period of 32 days with a harmonic at 16 days.

3. TESS PHOTOMETRY

From the MAST archive, we retrieved 120-second cadence PDCSAP light curves from sectors 23, 50, 51, and 52 (Jenkins et al. 2016) and 20-second PDCSAP light curves from sectors 50, 51, and 52 (Jenkins et al. 2021). We clipped 3σ outliers to remove periodogram-biasing signals such as flares. Figure 1 (top right) shows the clipped 120-s light curve from Sector 50.

To build a low-variance power spectrum estimate, we averaged the Lomb-Scargle periodograms from each TESS light curve, a procedure known as Bartlett's method (Bartlett 1948). Figure 1 (lower left) shows the result, which has a clear sequence of local maxima. The maxima are marked by vertical lines, and the frequency range within one Rayleigh resolution unit $\mathcal{R} = 1/T$ (where $T = 27$ days is the TESS light curve duration) of each maximum is shaded in light gray. The dark overlap regions cover frequencies within one resolution unit of two local maxima. The overlaps indicate that the local maxima are separated in frequency by $< 2\mathcal{R}$, which means they are not fully resolved (Godin 1972). However, some numerical experiments suggest that signals are adequately resolved at separation $1.45\mathcal{R}$ (e.g. Kovacs 1981), so we use the local maxima as the basis for further analysis.

Our hypothesis is that the local maxima in the TESS average periodogram reside at the rotation frequency and its harmonics. To estimate the rotation period, we find the frequencies of the local maxima by using finite differences to approximate $d\overline{\mathcal{P}}/df$ (Figure 1, lower-right), the first derivative of the average periodogram with respect to frequency. At local maxima, $|d\overline{\mathcal{P}}/df| < \epsilon$, where $\epsilon \ll 1$ is a tolerance. Our estimated rotation frequency f_r minimizes

$$\sum_{i=1}^{5} (f_i - i f_r)^2, \tag{2}$$

where f_i are the first five local maxima, marked with red dots in the lower-right panel of Figure 1.

The best-fit rotation period is 15.7 days, which is statistically indistinguishable from the 16.3-day value of Perger et al. (2017a). Although a 32-day period is undetectable in an average periodogram computed from 27-day light curves, the harmonic sequence in Figure 1 nonetheless supports the original rotation period estimate of ~ 16 days. Furthermore, when analyzing the concatenated 20-second cadence light curves from Sectors 50–52, in which a 32-day periodicity would be detectable, we do not find a periodogram peak near $f = 1/32$ day^{-1}.

4. CONCLUSION

A Welch's power spectrum estimate from the GJ 3942 RV time series of Perger et al. (2017a) and the RV–Hα magnitude-squared coherence show periodicities at 16 days and 32 days. We used TESS photometry to try and break the degeneracy between the two possible rotation periods. An average periodogram created from seven TESS light curves reveals local maxima at harmonics of 15.7 days, which is statistically indistinguishable from the 16.3-day period reported by Perger et al. (2017a). The TESS observations suggest that the true rotation period is ~ 16 days and the 32-day signal is a subharmonic. However, the TESS rotation detection is ambiguous, as the periodogram peaks that may constitute a harmonic sequence are not resolved from one another according to the Rayleigh criterion.

The time series analyzed in this article are available at doi: 10.17909/n4nm-2c49 and Perger et al. (2017b). The `Jupyter` notebooks to execute the analysis in this paper/to generate the figures in this paper is hosted at Github[1] and is preserved on Zenodo at doi: 10.5281/zenodo.14199669 (Fonseca & Dodson-Robinson 2024).

Work by AF was supported by NSF's Philadelphia AMP Post-Baccalaureate Research Experience for LSAMP Students Program (grant no. 2008197). Work by SDR was supported by NSF grant 2307978.

Facilities: HARPS-N, TESS

Software: astropy (Astropy Collaboration et al. 2013, 2018, 2022), NWelch (Dodson-Robinson et al. 2022)

REFERENCES

Anglada-Escudé, G., & Butler, R. P. 2012, ApJS, 200, 15, doi: 10.1088/0067-0049/200/2/15

Astropy Collaboration, Robitaille, T. P., Tollerud, E. J., et al. 2013, A&A, 558, A33, doi: 10.1051/0004-6361/201322068

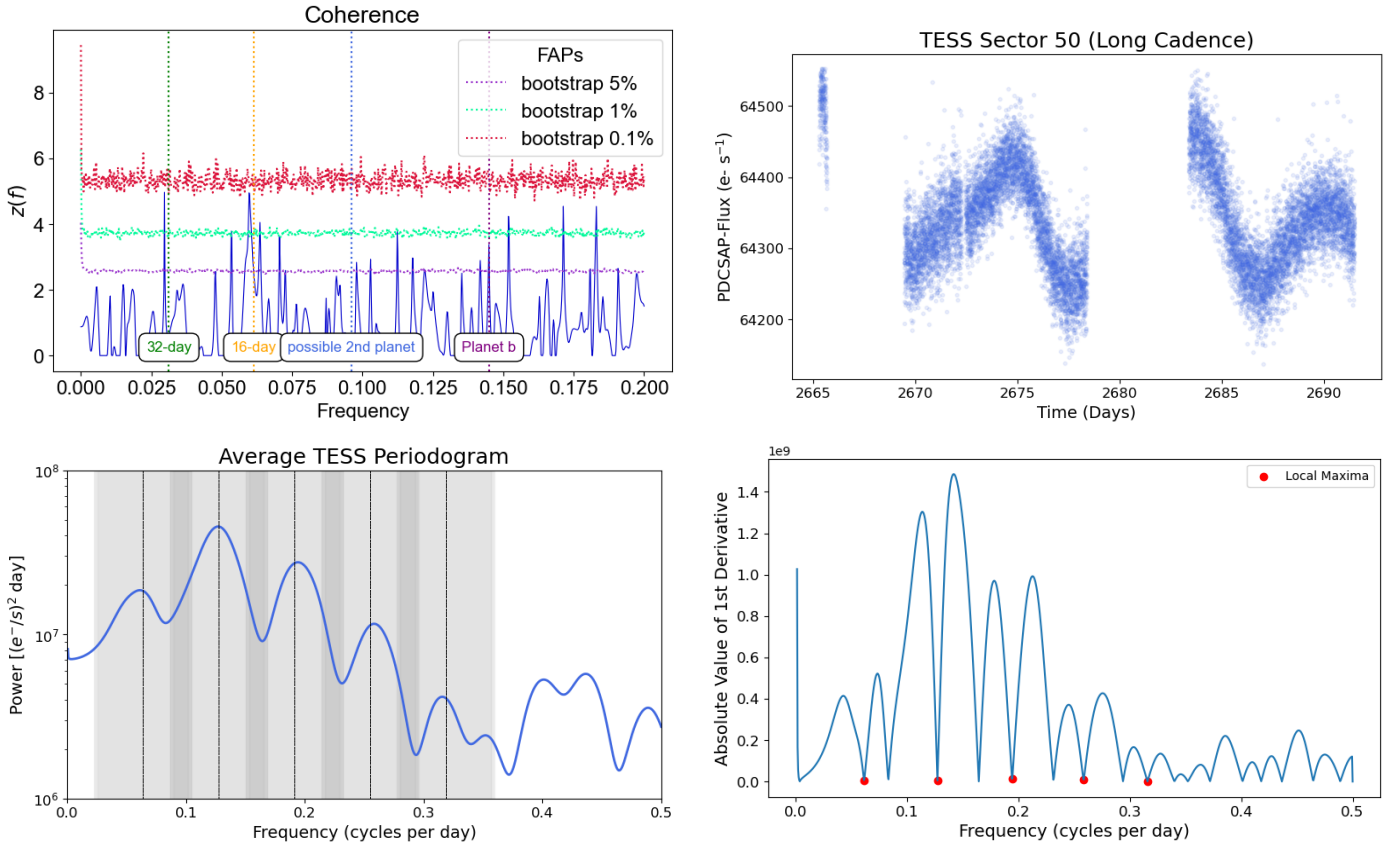

Figure 1. Top left: The Fisher-transformed magnitude-squared coherence estimate from RV and Hα has peaks at frequencies 1/32 day^{-1} and 1/16 day^{-1}. **Top right:** TESS PDCSAP photometry of GJ 3942 from Sector 52 shows evidence for rotational modulation. **Lower left:** Average periodogram from seven TESS light curves. Vertical lines indicate local maxima that may correspond to rotation harmonics. **Lower right:** $|d\overline{\mathcal{P}}/df|$ calculated from average TESS periodogram with probable rotation harmonics indicated by red dots.

Astropy Collaboration, Price-Whelan, A. M., Sipőcz, B. M., et al. 2018, AJ, 156, 123, doi: 10.3847/1538-3881/aabc4f

Astropy Collaboration, Price-Whelan, A. M., Lim, P. L., et al. 2022, ApJ, 935, 167, doi: 10.3847/1538-4357/ac7c74

Bartlett, M. S. 1948, Nature, 161, 686, doi: 10.1038/161686a0

Boisse, I., Bouchy, F., Hébrard, G., et al. 2011, A&A, 528, A4, doi: 10.1051/0004-6361/201014354

Dodson-Robinson, S. E., Delgado, V. R., Harrell, J., & Haley, C. L. 2022, AJ, 163, 169, doi: 10.3847/1538-3881/ac52ed

Fisher, R. A. 1929, Metron, 1, 3

Fonseca, A., & Dodson-Robinson, S. 2024, Time Series Analysis of GJ 3942, Zenodo, doi: 10.5281/ZENODO.14199669

Gaia Collaboration. 2020, VizieR Online Data Catalog: Gaia EDR3 (Gaia Collaboration, 2020), VizieR On-line Data Catalog: I/350. Originally published in: 2021A&A...649A...1G; doi:10.5270/esa-1ug, doi: 10.26093/cds/vizier.1350

Godin, G. 1972, The analysis of tides.

Gomes da Silva, J., Santos, N. C., Bonfils, X., et al. 2011, A&A, 534, A30, doi: 10.1051/0004-6361/201116971

Harris, F. J. 1978, IEEE Proceedings, 66, 51

Jenkins, J. M., Twicken, J. D., McCauliff, S., et al. 2016, in Society of Photo-Optical Instrumentation Engineers (SPIE) Conference Series, Vol. 9913, Software and Cyberinfrastructure for Astronomy IV, ed. G. Chiozzi & J. C. Guzman, 99133E, doi: 10.1117/12.2233418

Jenkins, J. M., Twicken, J. D., Caldwell, D. A., et al. 2021, in Posters from the TESS Science Conference II (TSC2), 183, doi: 10.5281/zenodo.5136731

Kovacs, G. 1981, Ap&SS, 78, 175, doi: 10.1007/BF00654032

Lépine, S., Hilton, E. J., Mann, A. W., et al. 2013, AJ, 145, 102, doi: 10.1088/0004-6256/145/4/102

Percival, D. B., & Walden, A. T. 2020, Spectral analysis for univariate time series (Cambridge University Press)

Perger, M., Ribas, I., Damasso, M., et al. 2017a, A&A, 608, A63, doi: 10.1051/0004-6361/201731307

—. 2017b, VizieR Online Data Catalog: HADES VI. GJ 3942b activity with HARPS-N (Perger+, 2017), VizieR On-line Data Catalog: J/A+A/608/A63. Originally published in: 2017A&A...608A..63P, doi: 10.26093/cds/vizier.36080063

Ramiaramanantsoa, T., Moffat, A. F. J., Harmon, R., et al. 2018, MNRAS, 473, 5532, doi: 10.1093/mnras/stx2671

Welch, P. 1967, IEEE Transactions on Audio and Electroacoustics, AU-15, 70